

1 Introduction

1.1 Motivation and Outline

Since the beginning of science, when there were only the four elements earth, air, fire, and water to distinguish, one was not only interested in the description of these elements, but rather in their interaction. Soon the investigation of reactions alone turned into the very prospering scientific field of chemistry. The impact of chemistry on technology and daily life was always strong and is nowadays stronger than ever: for example if one imagines the huge differences between a world before the emergence of synthetic materials and the world to day. These synthetic materials are the product of organic chemistry.

Most organic synthesis is normally performed in solution, which is reasonable because the physics of chemical reactions are governed by coulomb interactions of the participating atoms or molecular units. In contrast to gravitational interactions which are a typical bulk feature, these coulomb interactions are mediated through the surface of matter. Nevertheless, a lot of matter on earth is solid and chemistry on solid surfaces is central to many areas of practical interest such as heterogeneous catalysis, tribology, electrochemistry and materials processing. With the rise of surface sensitive techniques in the past decades [1], a lot of information and knowledge has been gathered on surface reactions. The adsorption and reaction kinetics of simple inorganic molecules of catalytical systems were extensively studied on single crystal model surfaces [2]. Especially the field of catalysis related surface science studies blossomed, because the industrial need for efficient chemical processes with both low energy consumption and low environmental impact has stimulated the quest for improved catalytic systems.

However, there are huge differences in reactions on surfaces compared to reactions in solution. First of all, the chemical reaction process on surface includes additional reaction steps. Reactants involved in a surface reaction in a first step have to adsorb on that surface and can even adsorb in a variety of different adsorption modes among which only a certain fraction is the chemical active adsorption mode. Furthermore, this first adsorption step is perhaps only an intermediate state for a reactant as e.g. H_2 , which further on has to dissociate to become chemically active. In a second phase the reactants have to meet on the surface that the reaction can proceed at all. In many systems this involves a specific place on the surface, the so-called active site [3], e.g. a step edge or a kink site along a step edge. Diffusion and by that complex molecule-substrate interactions play hence an important role during this step. Additionally, these molecule-substrate interactions may also lead to conformational changes of the reactants upon adsorption or may even induce surface reconstructions caused by the adsorbates.

Because the atoms of organic molecules are covalently bond, all chemical reactions have to entail bond forming, bond breaking or both. The actual reaction pathway therefore often involves a certain attack step where geometrical or sterical aspects play an important role. For example a π -double-bond can not be attacked by a substituent in the nodal plane of its constituting p -orbitals since they do not have any probability density in this plane. Due to the

restriction to two dimensions for reactions on a surface, steric hindrance is of more importance than in solution where the reactants can arrange freely in three dimensions. Therefore the conformational flexibility of larger molecules [4] plays an important role to overcome such steric hindrances. On the other hand, as will be seen in the Pt-cinchona chapter of this thesis, this conformational flexibility may also cause difficulties for experimental methods like STM in terms of resolution.

Finally, the reaction product has to desorb from the surface and its adsorption strength competes with the adsorption strength of new reactants, which try to adsorb on the surface, slowing down or even hindering this adsorption process. Also side products of the reaction might hinder the adsorption of new reactants. In catalysis this is known as poisoning and is a major issue for the longterm efficiency of a catalyst.

Only very recently, surface science studies in this field have been expanded to the study of the chemistry of relatively complex organic molecules on surfaces, in large measure in connection with the selective synthesis and catalysis of fine chemicals and pharmaceuticals (for an extensive review see Z. Ma and F. Zaera [5]). Although the major advances of catalysis were a consequence of mostly empirical trials, advances in the scientific understanding of catalytic systems contributed to further improvement. Therefore the motivation for the work presented in chapter 3 was to further complete the scientific picture of such a complex catalytic system, namely the Pt-cinchona system. This heterogeneous catalytic system can be used for the enantioselective hydrogenation of achiral reactants.

Another strong motivation for research in the field of organic molecules and organic reactions on surfaces is the fascinating idea of molecular electronics. In 1974 Aviram and Ratner proposed a rectifier consisting of a single molecule [6] and thereby marked the laying of the cornerstone of molecular electronics. They suggested that a molecule with a donor-spacer-acceptor structure would behave as a diode when placed between two metallic electrodes. With its basic ideas already established by Feynman in 1960 [7] molecular electronics seeks to use individual molecules to perform non-linear electronic functions as e.g. rectification, amplification or storage. Herein, the necessity of non-linearity for most electronic devices excellently coincides with the non-linearity of quantum mechanical effects which rule the physics of nanoscale systems.

For the same reason of non-linearity of quantum mechanical effects an important point is the reproducibility of such nanoscale systems in order to exactly define the energy levels involved in the functional mechanisms. Organic molecules are made up of covalently bond atoms and are therefore well-defined atomic systems. To use organic molecules as basic building blocks of molecular electronics thus is a natural choice because large amounts of organic molecules can be repeatedly produced with an exactly defined number of atoms and chemical structure. Additionally, the electronic properties of organic molecules can be fine-tuned by variation of certain substituents. A final step along the road to molecular nanoelectronics is then the ability to order the single devices into hierarchical structures forming an electronic circuit. Such ordering processes must follow the same reproducibility and scalability rules known from classical semiconductor electronics in order to be of technological relevance.

In this context it can be very interesting to investigate how reactions of organic molecules can be used to build up higher hierarchical structures by self-assembly [8] on a surface. For this purpose the STM is an invaluable instrument, because it uses the 3rd dimension perpendicular to the surface for an investigative access to the planar molecular structures and reactions on the atomic scale. The fact that STM creates a real-space image of the surface also excellently supports the investigation of sometimes complex hierarchical structures.

In the following, chapter 2 introduces the experimental methods and the instrumentation used in the course of this thesis. Since the work presented in this thesis is based on two distinct projects, chapter 3 and 4 both include their own motivation and conclusion section and can be read separately. Chapter 3 presents our results on a heterogeneous asymmetric catalytic system, the so-called Pt-cinchona alkaloid system. Chapter 4 shows the possibilities and limits of state-of-the-art self-ordering phenomena exemplified by means of a thermally induced surface-assisted reaction which then leads to the formation of highly ordered structures.

2 Experimental Methods

This chapter describes the experimental methods and tools used in this thesis with a special emphasis on scanning tunneling microscopy.

2.1 Scanning Tunneling Microscopy

2.1.1 Introduction

The invention of the scanning tunneling microscope (STM) about 25 years ago in 1981 by Gerd Binnig and Heinrich Rohrer [9] marked a milestone of surface investigation techniques. With the STM a new era of surface science was introduced, since this technique allowed for investigations of many different surfaces in real space with atomic resolution. Its impact on surface science was honored just five years later in 1986 when Binnig and Rohrer received the Nobel Prize for their invention. As the name implies, scanning tunneling microscopy is based on the quantum mechanical tunneling effect through thin energy barriers. In scanning tunneling microscopy a sharp conducting tip is brought into close proximity (in the order of a few Å) to a conductive sample. For the electrons in the two conductors the gap in-between represents an impenetrable energy barrier which cannot be overcome according to classical theory. But since electrons are quantum mechanical objects and the energy barrier is thin, electrons can tunnel through the barrier and give rise to a net tunneling current I in the nanoampere range if a small bias voltage is applied between tip and sample. To obtain a 2D image of the sample surface the tip is then scanned across the surface by piezo-electric actuators. While moving the tip, the corrugation of the sample surface induces variations of the tip sample distance z , which in turn drastically affects the tunneling current. As a rule of thumb, the current reduces by one order of magnitude for an increase of the gap distance by 1 Å. It is exactly this exponential behaviour that is the reason for the high lateral and - to some extent - vertical resolution of scanning tunneling microscopy, because around 90% of the tunneling current is passing through the topmost atom of the tip-apex, if we assume it protrudes about 1 Å further out than the other tip atoms.

Several modes of operation are used while scanning the tip across the surface. In the so called *constant height* mode the z distance is kept constant and the changes in I are measured. Another alternative mode—actually the one most frequently used—is the *constant current* mode, where a feedback system is used to adjust the tip sample distance z in order to keep the tunneling current constant at a certain current set point. In this mode the topographic information is therefore shifted to the feedback output signal z , which is acquired with a data acquisition system and fed to the z piezo-actuator. Generally, the *constant height* mode is used for fast scanning, but the sample has to be perfectly flat and thermal drift has to be small to prevent the tip from crashing into the sample. The *constant current* mode is safer and yields good resolution at the expense of lower scan speeds. The STM images presented in this thesis, for instance, have all been acquired in constant current mode, recording the

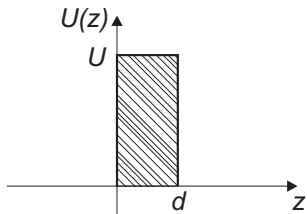
variation of the tip-sample separation which is then presented as a grayscale or color image.

Nowadays, the whole scanning operation and data acquisition is fully computer controlled, which means that scanning parameters like x - y scan speed, bias voltage and current set point are adjusted through computer interfaces. With the arrival of fast computers and field programmable gate arrays even the feedback system has become fully digital, which offers advantages in controlling certain feedback loop parameters, as e.g. the proportional and integral response of the feedback loop or the distance z in hold modes like I - V curves and scanning tunneling spectroscopy (STS) measurements.

2.1.2 Theory of STM

An exact treatment of the tunneling process in STM is virtually impossible, since this would require a detailed description of the quantum mechanical sample and the tip states and their evanescence into the tunneling gap. Especially the description of the tip states is impossible since the exact tip geometry and chemical composition are normally not known. Moreover, it is common knowledge that the tip structure, and hence also the resolution of the STM images obtained, may change during an experiment. Nevertheless, models and theories on different levels of approximation have been developed over the years. An overview of existing theories for the tunneling junction of STM can be found in textbooks [10, 11] or in a review article by Drakova [12].

A one-dimensional tunneling process serves as an elementary model in order to introduce the basic concepts and features of STM imaging. In classical mechanics, an electron with energy E moving in a piecewise constant barrier potential



$$U(z) = \begin{cases} 0 & \text{for } z < 0 \\ U & \text{for } 0 < z < d \\ 0 & \text{for } z > d \end{cases}$$

is described by

$$\frac{p_z^2}{2m} + U(z) = E$$

where m is the electron mass and p_z its momentum. If $E < U$ the electron has a nonzero momentum p_z in regions outside the barrier, but it cannot penetrate the barrier and is therefore confined to one side of the barrier. In quantum mechanics, however, the state of the same electron is described by a probability wavefunction $\psi(z)$, which satisfies the stationary Schrödinger equation

$$-\frac{\hbar^2}{2m} \frac{d^2}{dz^2} \psi(z) + U(z)\psi(z) = E\psi(z), \quad (2.1)$$

with the reduced Planck constant \hbar . In the classically allowed region $z < 0$,

$$\psi(z) = \psi(0)e^{+ikz} \quad (2.2)$$

with the wave vector $k = \sqrt{2mE}/\hbar$ is the solution of Eq. 2.1 for an electron moving in positive z direction. In the classically forbidden region—the barrier—the solution is

$$\psi(z) = \psi(0)e^{-\kappa z} \quad (2.3)$$

with the decay constant

$$\kappa = \frac{\sqrt{2m(U - E)}}{\hbar}. \quad (2.4)$$

Hence, the probability w of observing an electron at the end of the barrier at $z = d$ is

$$w \propto |\psi(d)|^2 = |\psi(0)|^2 \exp(-2\kappa d). \quad (2.5)$$

If we consider this potential as a model for the metal-vacuum-metal junction of our tunneling gap, the work function Φ of the metals plays the role of the potential barrier height U , assuming the work functions to be equal and neglecting the thermal excitation of the electrons in the metal. The electron can tunnel from one metal to the other and *vice versa*. However, without a bias voltage, there is no net tunneling current. By applying a bias voltage V , a net tunneling current occurs and we end up with a model like Fig. 2.1.

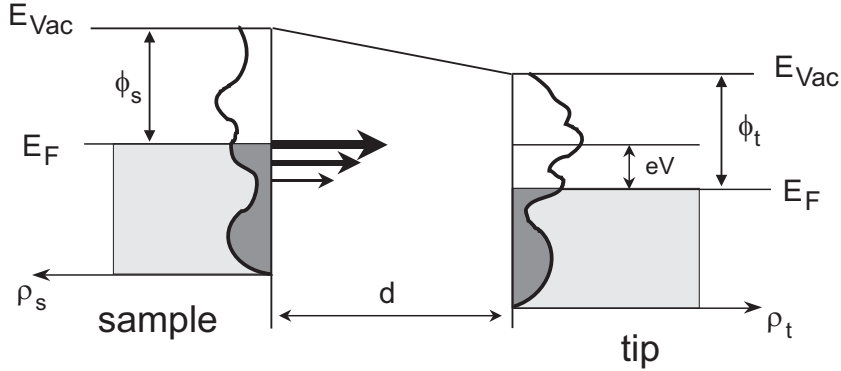


Figure 2.1: Schematic 1-dimensional diagram of a tip-sample junction. In this representation a negative bias U has been applied to the sample and electrons therefore tunnel from occupied sample states into unoccupied tip states. The size of the horizontal arrows indicates the different transmission coefficients (and therefore of the tunneling probabilities) for electrons of different energies.

Assuming $eV \ll \Phi$, an electron in the n th sample state ψ_n with the energy E_n between the Fermi level E_F and $E_F - eV$ has the probability

$$w \propto |\psi_n(d)|^2 = |\psi_n(0)|^2 \exp(-2\sqrt{2m\Phi}d/\hbar) \quad (2.6)$$

to be present at the tip surface. $\psi_n(0)$ is the value of the n th sample state at the sample surface and a summation over the total number of those states within the energy interval eV leads to the tunneling current

$$I \propto \sum_{E_n=E_F-eV}^{E_F} |\psi_n(d)|^2. \quad (2.7)$$

If eV is small enough so that the density of electronic states does not vary significantly within $[E_F - eV, E_F]$, the sum in Eq. 2.7 can be conveniently expressed with the *local density of states* (LDOS) $\rho_s(z=0, E_F)$ of the sample at the Fermi level E_F

$$I \propto V \rho_s(z=d, E_F) = V \rho_s(z=0, E_F) \exp(-2\sqrt{2m\Phi}d/\hbar) \quad (2.8)$$

According to the previous equation, a constant-current STM image at low bias voltages is a contour map of the sample surface LDOS at the Fermi energy and at the position of the tip

surface. Additionally the equation includes the exponential decay of the tunneling current I with increasing tip-sample distance d which, as already stated, is the main reason for the high resolution in STM.

As early as 1961, Bardeen [13] introduced a way to calculate the tunneling current between two planar metal plates in the context of metal-insulator-metal tunneling junctions. Instead of trying to solve the Schrödinger equation of the whole system, Bardeen considered two separate subsystems with a semi-infinite insulator first. He obtained the electronic wavefunctions for the separate subsystems by solving their stationary Schrödinger equations individually and then calculated the rate of the electron transfer by using time-dependent perturbation theory. This concept was first applied to the tip-sample geometry by Tersoff and Hamann in the so-called *s-wave approximation* [14, 15].

From Fermi's golden rule [16] the probability w of an electron to tunnel between a sample state ψ_s and a tip state ψ_t is

$$w = \frac{2\pi}{\hbar} |M|^2 \delta(E_{\psi_s} - E_{\psi_t}) \quad (2.9)$$

if only elastic tunneling is considered, i.e. only tunneling between states with the same energy $E_{\psi_s} = E_{\psi_t}$. As Bardeen already showed, the amplitude of electron transfer, or the tunneling matrix element M , is determined by the overlap of the surface wavefunctions of the two subsystems at a separation surface S_0 as

$$M = \frac{\hbar^2}{2m} \int_{S_0} (\psi_s^* \nabla \psi_t - \psi_t \nabla \psi_s^*) dS. \quad (2.10)$$

If a bias voltage V is applied the tunneling current is calculated by summing over all the possible states

$$I = \frac{2\pi e}{\hbar} \int_{-\infty}^{\infty} [f(E - eV) - f(E)] \rho_s(E - eV) \rho_t(E) |M|^2 dE \quad (2.11)$$

where $f(E) = [1 + \exp((E - eV)/k_B T)]^{-1}$ is the Fermi distribution function of the thermally excited electrons at temperature T and ρ_s and ρ_t are the densities of states (DOS) of the two electrodes. k_B is the Boltzmann constant. If $k_B T$ is smaller than the energy required in the measurement, the Fermi distribution can be approximated by a step function and the tunneling current becomes

$$I = \frac{2\pi e}{\hbar} \int_0^{eV} \rho_s(E_F - eV + E) \rho_t(E_F + E) |M|^2 dE. \quad (2.12)$$

If the tunneling matrix element $|M|$ does not change appreciably in the interval of interest, the tunneling current is determined by a convolution of the DOS of the two electrodes

$$I \propto \int_0^{eV} \rho_s(E_F - eV + E) \rho_t(E_F + E) dE. \quad (2.13)$$

Clearly, the electronic structure of the two participating electrodes is incorporated in the formula in a symmetric way and the two parts are interchangeable. If one DOS, e.g. the tip DOS, can be regarded as constant, the current scales with the DOS of the sample. Tersoff and Hamann now faced the difficulty of evaluating the tunneling matrix element M of Eq. 2.10

by approximating the tip as a protruded piece of metal, with spherical symmetry and radius R modeled in the jellium model. Among the different solutions of this quantum mechanical problem Tersoff and Hamann showed that for most problems the main contribution comes from the s-wave solution, lending their approach the name s-wave approximation. This solution yields the tunneling matrix element

$$M \propto \kappa R e^{\kappa R} \psi_s(r_0), \quad (2.14)$$

where $\kappa = \sqrt{2m\phi}/\hbar$ is the minimum inverse decay length for the wave functions in the vacuum gap with an effective local barrier height ϕ . $\psi_s(r_0)$ is the sample wavefunction at the center r_0 of the tip apex. Proceeding on all the assumptions made up to this point [17], this approach leads to the following current dependency for small bias voltages

$$I \propto V \frac{R^2}{\kappa^2} e^{2\kappa R} \rho_t(E_F) \rho_s(E_F, r_0), \quad (2.15)$$

with ρ_t being the DOS of the tip. As can be seen in equation 2.8 the tunneling current is proportional to the sample LDOS ρ_s at the Fermi level at the center of the tip apex. The exponential dependence on the gap distance d is again reproduced here, due to the exponential decay of the sample wavefunctions into the vacuum gap: $\rho_s = \sum_s |\psi_s(r_0)|^2 \delta(E_{\psi_s} - E_F)$ and $|\psi_s(r_0)|^2 \propto \exp(-2\kappa(R + d))$.

By assuming an s-wave for the tip, the approach of Tersoff and Hamann relates the tunneling current only to properties of the sample alone. A constant current image therefore reflects the contour of constant LDOS at the Fermi level of the sample. For metals the LDOS at the Fermi level almost coincides with the total electron density, because of the faster exponential decay of the energetically deeper lying occupied states. These surface charge density contours exhibit the periodicity of the surface atoms and directly reflect the surface topology.

2.1.3 Imaging Adsorbates with STM

One has to be aware that the simple topographic interpretation of constant current STM images of metal substrates does not hold true for single atom or molecular adsorbates¹. This is for instance seen for the imaging of O on Pt(111) [18, 19], which is counterintuitively imaged as a depression with respect to the bare metal surface. Another example is the imaging of CO on Cu(211) [20, 21] where CO can appear as both a depression or a protrusion, depending on the proximity of neighbouring molecules and the modification of the tip by adsorbed CO. Even in the case of large organic molecules with an extended π -electron system, the height interpretation is not necessarily straight forward as the example of porphyrin molecules shows [22]. These molecules are imaged as depressions or protrusions depending on their substituents.

Before the first successful STM images of organic molecules were reported [23–26], it was debated whether molecular imaging should be possible at all. The doubts stem from the fact that most organic molecules have a rather large energy gap between their highest occupied molecular orbital (HOMO) and their lowest unoccupied molecular orbital (LUMO). Since the tunneling current is proportional to the LDOS at the Fermi energy according to Tersoff and Hamann, the molecules should not be visible at low bias voltages. Adsorbate states far from

¹Even for clean metal surfaces the topographic interpretation is sometimes too simplistic, if one thinks of features like surface state images at step edges